Isr. J. Earth Sci.; 41: 9–20

Radon emanation along border faults of the Rift in the Dead Sea area

Gideon Steinitz,[1] Uzi Vulkan,[2] Barbu Lang,[1] Arie Gilat,[1] and Hovav Zafrir[2]

[1]Geological Survey of Israel, 30 Malkhe Yisrael Street, Jerusalem 95501, Israel
[2]Soreq Nuclear Research Center, Yavne 70600, Israel

(Received 1 January 1992 and in revised form 9 September 1992)

ABSTRACT

Steinitz, G., Vulkan, U., Lang, B., Gilat, A., Zafrir, H. 1992. Radon emanation along border faults of the Rift in the Dead Sea area. Isr. J. Earth Sci. 41: 9–20.

Radon anomalies along the western shore of the Dead Sea, previously reported only from springs in the area, are also traceable in the sediments and rock units in the area. The anomalies, of up to several thousand pCi/l, are not supported by local uranium.

The recorded spatial extension of one of the radon anomalies, in the Enot Zuqim area, reaches up to 3 km in a north–south direction, along the strike of the major structural elements, and up to 1 km perpendicular to them. The radon values in the regional anomaly are up to 10 times the background values. Local anomalies are superimposed on the regional anomalies. Some of these secondary features are associated with "freshwater" springs flowing out from the young graben fill. A second type of superimposed high anomaly is associated with the large north–south-trending faults which are major structural elements of the Rift. At these localities the radon anomaly itself is located in the Rift sediments next to the fault scarp.

Systematic temporal fluctuations (5 times local background) in the radon flux have been recorded at a very high radon anomaly at Enot Zuqim. The peak duration measured to date is in the order of 10 days. Such a variation precludes a near-surface source for the radon, such as secondary uranium or radium concentrations.

The extent of the features traced suggests that along the western boundary fault of the Rift, a radon complex is developed consisting of:

a. *A source rock emanating radon at a high concentration*, extending over considerable stretches, at an unknown depth. The downfaulted Senonian phosphorites, containing 100-120 ppm uranium are a possible source.
b. *A transport mechanism*, probably of a convective nature, enabling the rapid ascent of radon to the surface.
c. *A conduit system* which is apparently connected with the large structural elements as well as to the hydrologic system operating along the Rift boundaries.

INTRODUCTION

The use of radon as a geochemical tracer has been developed primarily in connection with uranium prospection, environmental research, and earthquake prediction (Durrance, 1986). Its behavior has been investigated in natural waters, in unconsolidated sediments (soils), and in rocks. One of the major aspects addressed in these studies is the distance of transport of radon and the processes involved.

Radon (Rn^{222}), an alpha-emitting noble gas, is produced in the radioactive decay series of uranium (U^{238}). Being a gas it has the ability to migrate from its source, mainly upwards. The presence of radon, away from its uranium source, is controlled by a combination of its emanation power, its mobility, and by its half life (3.8

0021–2164/92 $4.00

days). This unique combination of features underlies the interest in radon as a geochemical and geophysical tracer.

Emanation power of radon (Tanner 1964, 1980) refers to the fraction of total gas that escapes from the host mineral to the pores in the rock. It varies from less than 1% to 20–30%. Barretto (1975) proposed an average value of 7% for granites.

Following its emanation into the rock pores, radon can be transported by diffusion or by other mechanisms — mainly convection. It is evident that diffusion alone cannot account for radon transport beyond several meters. Mogro-Campero and Fleischer (1980) postulated a theory of underground fluid convection, driven by local thermal gradients, in order to account for presumed radon migration to a distance of 100 meters and more. Kristiansson and Malmqvist (1982) also suggested similar distances for upward flow of radon. Pacer and Czarnecki (1982) measured anomalous radon concentration in the unconsolidated cover sediments over known uranium mineralization, up to 140 meters above the ore body.

The use of radon as an earthquake precursor was investigated extensively during the last decade in a variety of geological settings. Papastefanou et al. (1989) reported that each earthquake with magnitude ≥ 4.0 and epicenter within 50 km of the monitoring site was preceded by a radon anomaly. Ramola et al. (1989) reported on radon anomalies preceding earthquakes, detected during systematic radon measurements in soil and water sources.

Radon concentrations of up to 21,000 pCi/l (picocuries per liter of pore air) (Mazor, 1962) and 89,000 pCi/l (Kronfeld et al., 1991) have been encountered in water sources along the Dead Sea Rift. Since the mid-1980s an ongoing project has been undertaken to measure the radon content of various rock units in Israel. The early phase was connected with uranium prospection (Strull et al., 1986; Vulkan et al., 1991). Recent geochemical and geo-environmental invesigations led to mapping the radon content in Cretaceous and Tertiary formations in the northeastern Negev, some 30 km to the west of the Dead Sea (Shiloni et al., 1991). Based on this survey, radon concentrations of 80–100 pCi/l of rocks containing 1–2 ppm uranium are herein referred to as background values for the sedimentary rocks of the region.

The Dead Sea Rift (Transform) is a major tectonic feature in the area. Its subrecent and present activity has been extensively studied geologically, geomorphologically, and seismically. The present radon survey, conducted in the Dead Sea area, was aimed at determining a possible connection between eventual radon anomalies and geological features related to the recent tectonic activity. The aim was to try to trace the radon anomalies, so far reported in some water sources only, by measuring radon in a variety of geologic situations. The survey was initiated in 1990 and a preliminary report was given by Vulkan et al. (1991).

GEOLOGICAL SETTING

The Dead Sea basin is situated in the most prominent rhomb-shaped graben developed along the Dead Sea Rift. This rift is viewed as a transform fault system, developed in the Tertiary and Quaternary in association with the opening of the Red Sea (e.g., Garfunkel 1981, Quennell 1983). The Dead Sea is bounded by two large north–south major border faults which are first-order structures of the Dead Sea Rift. The age of faulting is constrained, in this sector, by a variety of stratigraphic, geomorphologic, and related criteria. Clear evidence for Rift-related tectonics in the area are recorded from the Miocene onwards (e.g., Picard, 1943; Steinitz and Bartov, 1991). The faults are grouped, for the present purpose, as follows:

a. The *eastern border fault* has the largest vertical offsets. This boundary fault is the major fault of the Dead Sea Rift in this sector, exposing Precambrian basement at the base of the fault scarp, and raising the Tertiary continental peneplains, immediately to the east, to elevations of more than 1400 meters. This fault zone was not investigated here.
b. The main *western boundary fault* is a roughly north–south-trending normal fault. It is well exposed along considerable stretches of the Dead Sea shore. At a level close to the shoreline the western (upthrown) block exposes a prominent fault scarp composed of the Cenomanian Judea Group dolomites. The downfaulted block is rarely exposed. It is usually covered by the young, unconsolidated, graben fill.
c. *Subsidiary north–south-trending faults* are developed within the structural block to the west of the main western boundary fault.
d. *Intra-Rift faults* are observed in the young Rift sediments and the subrecent clastic sediments along its boundaries. North–south-trending faults, parallel to the main Rift faults, cut the Upper Pleistocene Lisan Formation along the western fault scarp as well as in the central part of the valley — north of the Dead Sea

and east of Jericho. A long diagonal fault of similar age cuts across the Rift Valley a few kilometers south of the Dead Sea. A special feature in this respect is the fault-bounded Mount Sedom salt plug, which is moving upwards in the southwestern corner of the Dead Sea.

The Dead Sea sector of the Dead Sea Rift exhibits abundant geological evidence for very recent tectonic activity (Gardosh, 1987). The most noteworthy are the post-Lisan-Formation (Upper Pleistocene) faults. The present tectonic activity of the Dead Sea area is clearly indicated by the ongoing seismicity (cf. Ben-Menachem, 1979; IRPG, 1991; Turcotte and Arieh, 1986).

A series of surveys of the radium and the radon concentrations of Israeli water sources were conducted in the 1950s. The results were extensively described by Mazor (1962). Radon anomalies, unsupported by radium, were found in various sources along the Rift Valley, particularly in water sources along the western shore of the Dead Sea. It was suggested by Mazor (1962) that these anomalies are connected with underground reservoirs of brines, oils, and gases.

Kronfeld et al. (1991) described radium deposition at and near active and relict springs along the Dead Sea coast. They associated the elevated radon anomalies found in the spring water with the radium that precipitated from the water and concentrated in the spring sediment. As a source for the radium they suggested the Dead Sea itself.

METHODS

The alpha track ("track etch") method was utilized in the present study. It is a simple and integrative method that was developed and widely used, primarily for uranium exploration (Fleischer et al., 1975, 1980; Gingrich and Fisher, 1976; Kristiansson and Malmqvist, 1982, 1984; Mogro-Campero and Fleischer, 1980; Ramola et al., 1989; Wattananikorn et al., 1990). It is generally employed in soils covering the rock formations from which the radon is assumed to migrate. In arid zones soil cover is often meager and measurement must be carried out directly on rocks. The technique and efficacy of utilizing the method on rocks has been demonstrated by Strull et al. (1986), Vulkan et al. (1991), and Shiloni et al. (1991). The analytical method is documented in detail by Steinitz et al. (1992).

In order to find optimal depths and times for burying the film canisters, tests were run. It was found that the optimal conditions required that the films be buried at a depth of 50 cm. In order to measure the radon level over time, modifications in the measurement setup were made. A rope was attached to the plastic cup (containing the sensor film) to enable easy in situ replacement of the cup in the PVC pipe which remained in the ground. The duration that the film was kept in the ground at a specific site depended upon the local radon levels. In areas of high radon, the plastic films were collected after several days. In cases of low radon emanations, long measurement times, up to 28 days, were needed. Gamma-ray spectroscopy using a NaI(Tl) crystal, was used to determine the equivalent uranium concentration at the site (50 cm depth) of radon measurement.

SAMPLING

Location of the sites is given in Fig. 1. The sampling was conducted in three successive stages:

1) The first stage consisted of sampling a series of 13

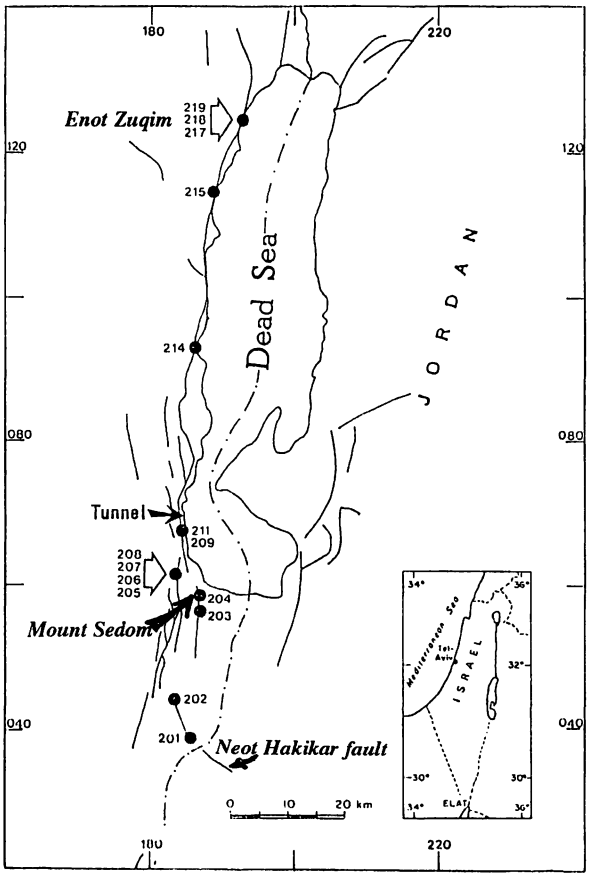

Fig. 1. Location map. Numbers refer to the sampling sites as given in Table 1.

sites distributed along the western side of the Dead Sea. The sites examined included a diagonal fault within the Rift just south of the Dead Sea, the Mount Sedom salt plug, faults within the marginal zone, areas next to springs with reported radon anomalies, and sites next to major faults. The sampling was targeted to trace radon anomalies in the sedimentary units at the Rift border and in the Rift fill.

2) In light of the results obtained in the first stage, further sampling was concentrated around the En Gedi spring area and a number of sites in the Enot Zuqim area. The aim was to obtain a better appreciation of the areal extent of the anomalies encountered in the first stage.
3) The high anomaly encountered at Enot Zuqim was studied in greatest detail. Monitoring was repeatedly carried out in order to observe whether the radon emanation varies over time.

At all sampling sites it was attempted to space the individual sample points approximately 20 meters apart. The actual distances between adjacent points varied between 5 and 20 meters. The factors determining the density utilized were both statistical (minimum sample number required as a function of the expected variation) as well as the local geological and/or the topographic conditions.

RESULTS

The radon survey was carried out over 7 geographical sites (Fig. 1), listed below from south to north. The mean, standard deviation, and range of the radon emanation at each site are presented in Table 1.

Similar mean gamma radiation levels, in the range of several tens of CPS, were recorded in the different sites. Such values are typical of the background levels as observed in regional radiometric surveys in Israel. In none of the sites described below could a correlation be established between the local gamma radiation and the radon content.

1. Neot HaKikar fault (sites 201, 202)

The Neot HaKikar fault is developed south of the Dead Sea (Fig. 1). It trends WNW–ESE, diagonal to the Rift. The fault trace extends for several kilometers and cuts across the Late Pleistocene Lisan Formation. The southern block is elevated several tens of meters. A series of springs are developed along the fault scarp. Relatively high radon contents (up to ca. 1000 pCi/l) have been previously reported in these waters by Mazor (1962).

Two traverses were sampled roughly perpendicular to the trace of the fault. The distance between the traverses was 5 kilometers. At each traverse sampling tubes were placed on each side of the fault. Overall, the radon concentrations detected over the two traverses are close to the background values or slightly higher. No difference could be discerned between the two sides of the fault, nor is any radon anomaly encountered along the fault trace.

2. Mount Sedom (sites 203, 204)

Two sites were investigated along the Pleistocene salt diapir of Mount Sedom. The sites were placed on its western side, at the base of the evaporite outcrop. The radon levels are among the lowest encountered (100 ± 50 pCi/l), all in the range of background radon levels. This is to be expected due to the low uranium content of the salt, as well as to the low porosity and low diffusion of liquid and gas in the salt layers.

3. Nahal Hemar (sites 205, 206, 207, 208)

Nahal Hemar is a deep gorge incised, several kilometers westward, into the Rift shoulder just north of Mount Sedom. The country rocks are mainly subhorizontal carbonates of the Cretaceous Judea and Mount Scopus groups. Structurally the area is typified by a series of large N–S-trending faults belonging to the marginal faults of the Dead Sea Rift, developed in the block bounding to the west the Rift proper. The faults display large normal throws, evidenced by stratigraphic separations of several hundred meters (Agnon, 1983). The last activity on these faults predates the deposition of the Lisan Formation. Nahal Hemar exposes these faults at the wadi bed level, at an elevation which is approximately 100 meters above that of the Dead Sea.

The sites for measuring the radon content were located on large faults and on larger tectonic zones. The sampling points streched across a lineament to a distance of tens of meters from each side of its trace. In most locations the sampling tubes were buried in the wadi gravel, up to a few tens of centimeters thick, as near as possible to the underlying bedrock.

The radon levels encountered are typical of those for the country rocks. Cenomanian limestones and dolomites gave the lowest values (63 ± 34 pCi/l), in accordance with the very low (< 1–2 ppm) uranium content in them. Measurements on Senonian strata, on a down-faulted block across the fault, showed somewhat higher values (ca. 200 pCi/l) which are in the range expected for the Senonian chalky and phosphatic beds in accordance with their higher uranium content (Shiloni et al., 1991). Thus, all variation in radon content across struc-

Table 1. Radon concentrations at sampling sites

Site	Location	Coordinates	#	Radon	
				mean ± S.D. (pCi/l)	range (pCi/l)
201	Neot HaKikar	1851/0391	16	100 ± 34	45–163
202	Neot HaKikar	1832/0445	20	146 ± 41	86–218
203	Mount Sedom	1876/0551	5	110 ± 102	12–255
204	Mount Sedom	1870/0580	10	90 ± 33	56–164
205	Nahal Hemar	1818/0608	10	63 ± 34	20–117
206	Nahal Hemar	1827/0610	10	261 ± 122	29–499
207	Nahal Hemar	1829/0612	8	174 ± 44	112–213
208	Nahal Hemar	1831/0615	6	84 ± 15	63–104
209	Nahal Boqeq	1840/0674	12	151 ± 150	37–561
211	Nahal Boqeq	1840/0674	10	221 ± 76	103–319
214-1	En Gedi Spa	1862/0922	10	372 ± 89	275–600
214-3	En Gedi Spa	1862/0922	9	303 ± 155	123–623
214-I	En Gedi Spa	1862/0922	15	508 ± 202	267–917
214-II	En Gedi Spa	1862/0922	15	546 ± 414	138–1337
214-III	En Gedi Spa	1862/0922	15	430 ± 101	265–588
214-IV	En Gedi Spa	1862/0922	10	207 ± 111	109–436
215-I	Enot Qane	1889/1130	10	396 ± 185	114–754
215-II	Enot Qane	1889/1130	10	184 ± 130	44–440
217 old	Enot Zuqim, Traverse A	1926/1244	5	1169 ± 532	66–1896
217 new	Enot Zuqim, Traverse A	1926/1244	35	3514 ± 3783	42–12745
218	Enot Zuqim, Traverse B	1926/1253	43	273 ± 240	99–1476
219	Enot Zuqim, Traverse C	1933/1274	41	696 ± 404	149–1579

— number of samples.

tural elements in this zone can be seen as reflecting only the local lithological break across the fault, at the outcrop.

4. Nahal Boqeq (site 209, 211)

As it reaches the Dead Sea area, the Nahal Boqeq gorge exposes the Rift's main western fault. At this location the slightly eastwardly dipping massive dolomite beds, of the Cenomanian Hazera Formation, have been deeply incised by the wadi (Fig. 2). To the east of the fault, at this location, the steeply eastwardly dipping Senonian strata (Mishash, Ghareb, and Taqiya formations) are exposed on the downfaulted block. The faulting predates the Late Pleistocene Lisan Formation.

Two water sources are found in this area — En Noit and En Boqeq. At En Boqeq "freshwater" (ca. 1500 mg TDS/l; Mazor, pers. comm.) seeps out, from the Cenomanian carbonates, just to the west of the main fault, over a distance of several tens of meters. The En Noit spring (ca. 6600 mg TDS/l; E. Mazor, pers. comm.) is situated some 100 meters north of En Boqeq and several tens of meters higher in elevation. It is located east of the fault, but close to its trace, upon the Senonian strata of the downfaulted block. Mazor (1962) reports radon concentrations of 350 ± 20 pCi/l in spring water at En Boqeq and 2750 ± 70 pCi/l in the En Noit water.

Radon emanating from these rocks was measured at En Boqeq, along the wadi bed and across the fault (Fig. 2). The average radon emanation level determined for 9 samples sited upon the Cenomanian carbonates, just to the west of the fault, is 184 ± 160 pCi/l. Excluding three samples, believed to have been extracted by passersby, the average radon emanation is 240 pCi/l. Three other samples, placed immediately east of the fault, exhibit a much lower level of radon emanation, averaging 50 pCi/l. In spite of the relatively high standard deviation, the lithological and structural break across the fault is reflected in the comparative radon emanation levels. Morever the radon emanation encountered over the Hazera Formation dolomites (up to 561 pCi/l) is significantly higher than that which would be expected (<100 pCi/l) for rocks having a uranium concentration of approximately 1 ppm (Shiloni et al., 1991). The radon values encountered are therefore anomalous.

A further group of 10 samples was placed further east and downstream, on a wadi terrace which overlies steeplydipping Senonian chalks and marls. The terrace is several meters thick and is composed mainly of lime-

stone and dolomite pebbles derived from the upthrown block to the west of the fault. The source rocks of the terrace components have a low uranium content, reflected also by the low gamma radiation (74 ± 7 cps) measured on the terrace. However, the average radon level monitored within the terrace sediments is relatively high, 220 ± 76 pCi/l. It is presumed that the radon source is in the underlying lithology. It remains open at this stage whether a higher anomaly, unsupported by local uranium, exists in the underlying strata or whether the radon levels originate from the uranium-bearing Senonian phosphates buried at a shallow depth.

5. En Gedi Spa (site 214)

The En Gedi Spa sampling site, located a few hundred meters north of the En Gedi Spa, was placed on the gravels and old shorelines padding the plain exposed by the gradually receding Dead Sea. A 200-meter-long east–west traverse was sampled on this plain (Fig. 3). The western end is situated next to the main road, some 150 meters east of the morphologic scarp of the Dead Sea valley. Four lines of samples, directed N–S, were carried out. Samples were spaced 50 to 100 meters apart. Within each line two rows of samples were placed. The eastern group (214-I) is close to "freshwater" sources seeping out of the gravels. The Dead Sea shore was situated, at the time of the sampling, ca. 250 meters further to the east. A difference in elevation of 15 meters exists between the eastern and western ends of the traverse.

The En Gedi site exhibits a wide range of radon emanation values. The mean values are all above background values. The average values increase from west (200 pCi/l) to east (500 pCi/l). The eastward rise in the radon content is accompanied by a rise of the surface gamma radiation close to the "freshwater" seepages. The rest of the area has a normal background gamma radiation level. An additional line of samples was measured in the first phase (see Fig. 3, line 214-3). This line was positioned, diagonally, close to line 214-III. The mean radon content was some 30% lower.

At the En Gedi site a radon anomaly was found that extends over an area of 350 m × 150 m. The sampled area was chosen randomly on the roughly 1000 m × 2500 m plain, north of the Spa. Thus, it can be assumed that the anomaly (up to 10 times background) probably extends considerably beyond the investigated area. Within the anomaly a rise in the radon content is ob-

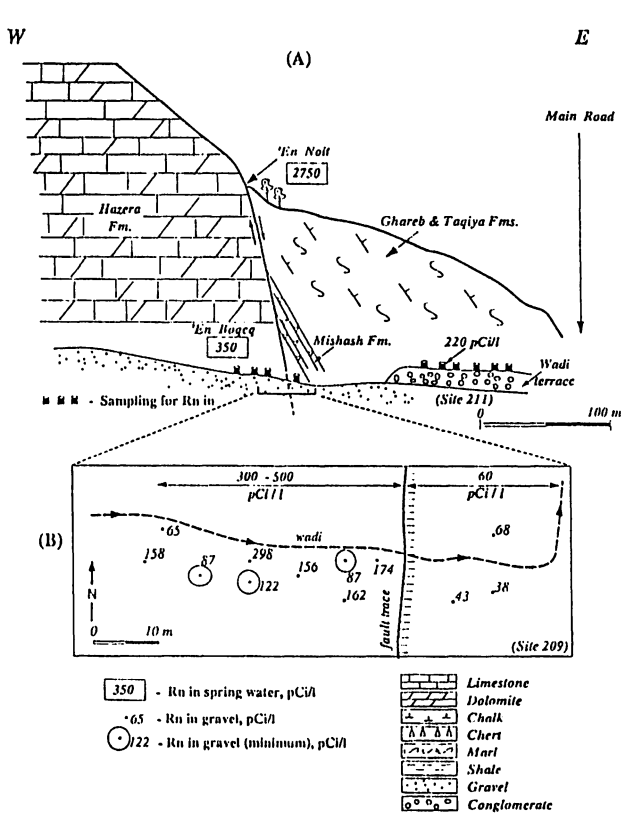

Fig. 2. Nahal Boqeq (sites 209,211): Radon results presented on cross section (A) and sampling map of site 209 (B).

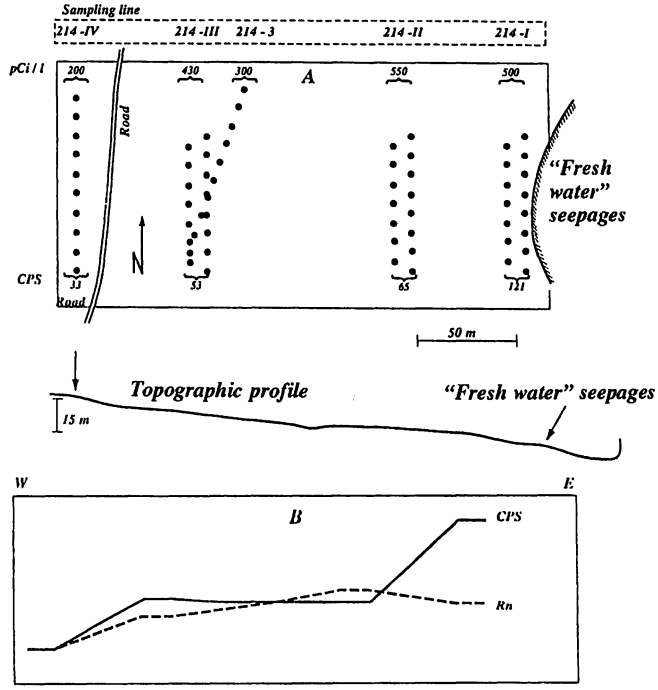

Fig. 3. En Gedi Spa (site 214): A — Distribution of samples and results along traverse. Line numbers (I–IV) refer to data in Table 2. For each line, radon values(pCi/l) and gamma radiation (CPS) are shown. B–Schematic variation (qualitative) of radon concentration and surface gamma radiation along the site.

served down the topographic gradient and with the approach to the "freshwater" seepages.

6. Enot Qane (site 215)

Enot Qane are a series of "freshwater" (100–7000 mg TDS/l, E. Mazor, pers. comm.) springs, spread over a N–S-trending strip (~1 km long and several hundred meters wide) between the main fault scarp and the Dead Sea shore. Two sampling stations were measured in the first phase of investigation. Both were east of the main road, on the lower part of the scree fan deposited at the base of the fault scarp. The eastern sampling pad (10 samples) was located close to the vegetation of Enot Qane, i.e., very close to the local water table. A radon level of 400 ± 185 pCi/l was measured on this pad. The second pad (10 samples), approximately 20 meters higher and 200 meters to the NW, located on the dry scree fan, yielded a radon level of 180 ± 130 pCi/l. In both pads background values of gamma radiation were measured at the surface.

7. Enot Zuqim (sites 217, 218, 219)

The highest radon anomalies were encountered at the Enot Zuqim area, situated in the northwestern sector of the Dead Sea. The area investigated, some three kilometers long and one kilometer wide, stretches in a north–south direction along the western shore. To the west it is bounded by the steep cliffs of the western fault of the Dead Sea Rift. Eastwards it extends to the "freshwater" sources seeping out from the alluvial fans which grade into the gravels of the Dead Sea shore.

The north–south-trending fault is the major structural element in the area, being the western boundary fault of the Rift in this area (Rot, 1970). The vertical separation on the fault is not known, but exceeds 500 meters. It may well reach 1 kilometer and more. The prominent fault scarp exposes, at the level of the Dead Sea, massive subhorizontal dolomite strata of the Cenomanian Hazera Formation. Obvious large fault plane surfaces are exposed at the base of the cliff. Slivers of the Plio-Pleistocene 'En Feshka Conglomerate (Mor, 1987) locally line the fault zone. Lacustrine marginal facies sediments of the Upper Pleistocene Lisan Formation were deposited, with an onlap, onto the fault scarp. Gullies and wadis, running down from the cliff, erode the soft Lisan Formation sediments and deposit gravels at the erosional base level. Local radium accumulations (12–547 ppm Ra eU) were reported from calcareous travertines enriched with Mn+Fe deposited in both the Judea Group carbonates and the Dead Sea Group conglomerates (Kronfeld et al., 1991).

Some of the radon sampling sites were located next to the base of the fault scarp. Others were placed close to the "freshwater" springs. The area between these elements was surveyed along three E–W traverses.

Traverse A (site 217). At this site (Fig. 4), covering an area roughly 50 m × 200 m, sampling was done as follows:

a. In the gravels and silt next to the base of the fault scarp. The area is dry but scrub vegetation indicates a near surface "freshwater" table (several meters ?). Two sampling lines of five tubes each were placed a few meters from the fault;
b. A series of tubes were buried along the trace of the fault, where it intersects a talus cone deposited against the scarp, to an elevation of some 10 m above the base of the scarp. All sampling tubes were located on the talus;

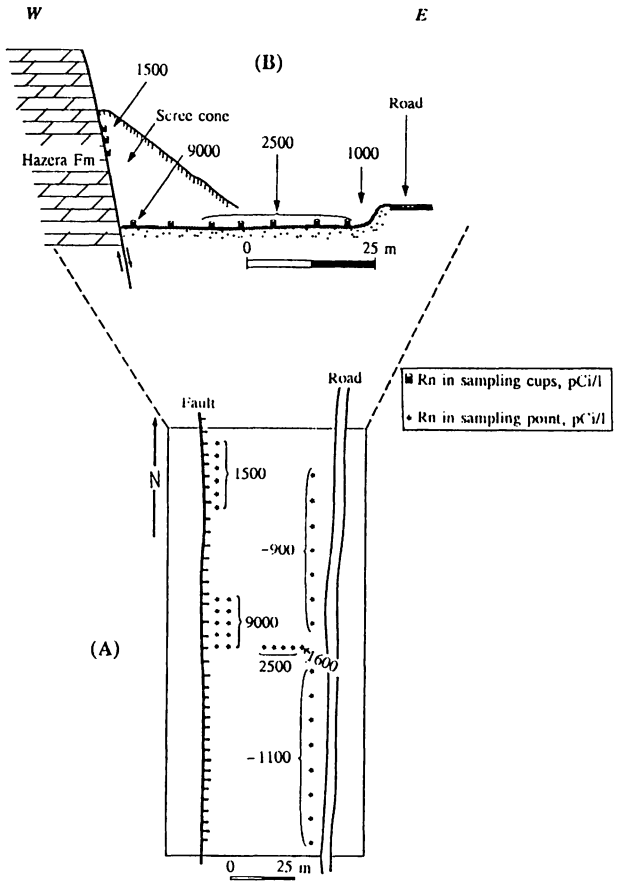

Fig. 4. Enot Zuqim — traverse A (site 217): Radon sampling map (A) and geological traverse with average radon levels (B). Legend — see Fig. 2.

c. Along a 50-m E–W traverse from the base of the scarp (A) to the main road;
d. On a 100-m N–S traverse placed some 50 m east of the fault.

All samples of Traverse A yielded high radon levels. They define an intense radon anomaly over the whole area (10,000 m^2). The mean of all 35 samples is 3510 ± 3800 pCi/l. The variation within the site follows the sampling pattern described above. The highest values of more than 12,000 pCi/l (average of 9060 pCi/l) were obtained in the gravels next to the base of the fault scarp. An anomalous flux of radon, reaching around 1500 pCi/l, is also traceable in the talus cone along the trace of the fault. A sharp decrease (by a factor of 8–10) is obtained at a distance of 50 m from the fault. This level, around 1000 pCi/l, could be traced along some 150 m in a N–S direction.

Traverse B (site 218). A continuous E–W traverse, some 500 m long, was measured north of the entrance to Enot Zuqim springs (Fig. 5). The western end of the traverse rests on the exposed base of the main western fault of the Dead Sea Rift. Here again a group of tubes was placed in the gravel next to the base of the fault scarp. From this point a series of sampling tubes were dispersed along the wadi bed and further on to the east, up to the vegetation developed at the "freshwater" seepages of Enot Zuqim springs.

At Traverse B the samples grouped around the fault scarp yield an anomalous radon concentration, around 250 pCi/l. Averaging the radon concentrations along the traverse, a slight decrease of the anomaly level is observable over the 350 m of the traverse. As in other cases, the variability of the values is high. Still most of the values are significantly anomalous (2–3 times background values). Along this traverse the topographic elevation decreases, to the east, ca. 20 m. A sharp jump (by a factor of 10–15) in the radon emanation is observed as "freshwater" seepages are approached.

Traverse C (site 219). The northern traverse, in an E–W direction, follows the wadi bed just south of Qumran (Fig. 6), approximately 1000 m northwest of Enot Zuqim springs. The wadi is incised into Lisan Formation sediments which are also deposited on the fault scarp. The western end is situated at the base of the main fault scarp where a group of samples were placed. From this point the traverse follows some 700 m eastwards and was sampled at a 20-m interval. No indication is found (vegetation) for "freshwater" at a shallow depth in the sampled zone. It is assumed that the level of such waters at the western end of the traverse is, at a minimum, several meters below the surface.

Along Traverse C a conspicuous radon anomaly of 1,500 pCi/l is found at the main N–S fault of the Rift. Eastwards, along the whole length of the traverse anomalous radon in the range of 700 pCi/l is observed. It is evident that a large (1000 m in E–W direction) radon anomaly exists in the young sediments of the Rift in the area. A sharp local radon anomaly is associated with the major Rift fault.

8. Monitoring the radon emanation at site 217

The extremely high radon anomaly encountered next to the fault scarp at Enot Zuqim was monitored repeatedly. The aim was to see how the anomaly varied over time. Two rows of samples, placed at the base of the fault scarp (Fig. 4) were measured several times, at varying intervals. The first measurement, in 10/90, used the normal sampling setup (removable PVC pipes). On 7/91 a new arrangement was emplaced consisting of 10 sampling pipes which permitted replacing the film without removing the pipes themselves. The duration of the first measurement was four days. Two successive measurements, of two days each, were performed in 8/91. Seventeen successive measurements, each of 2–3 days duration, were performed starting 3/10/91.

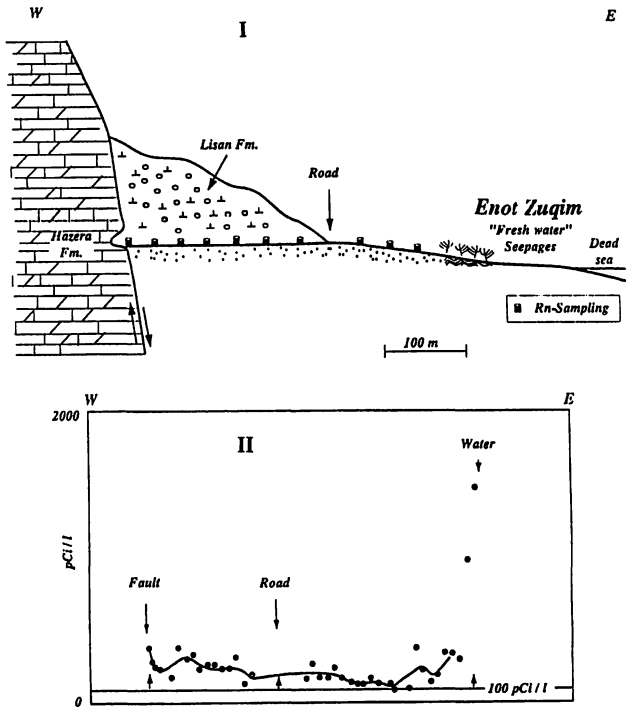

Fig. 5. Enot Zuqim — traverse B (site 218): Geological traverse (I) and radon levels along it (II). Legend — see Fig. 2.

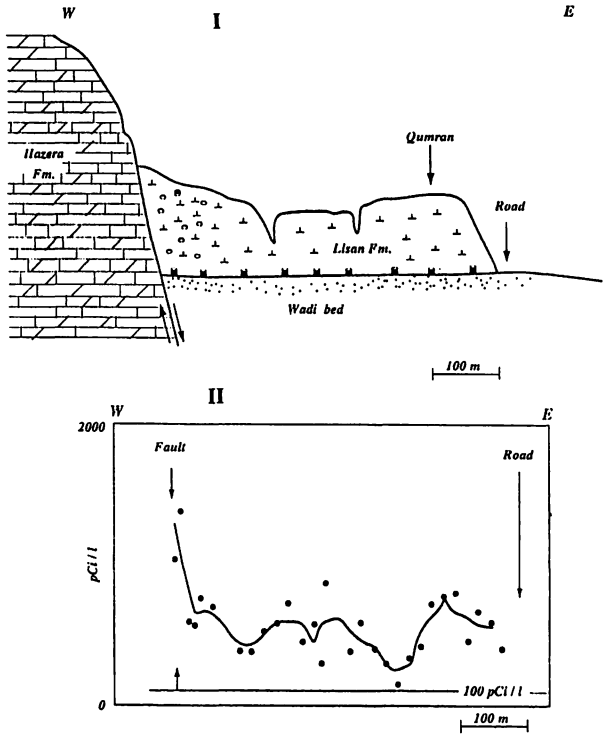

Fig. 6. Enot Zuqim — traverse C (site 219): Geological traverse (I) and radon levels along it (II). Legend — see Fig. 2.

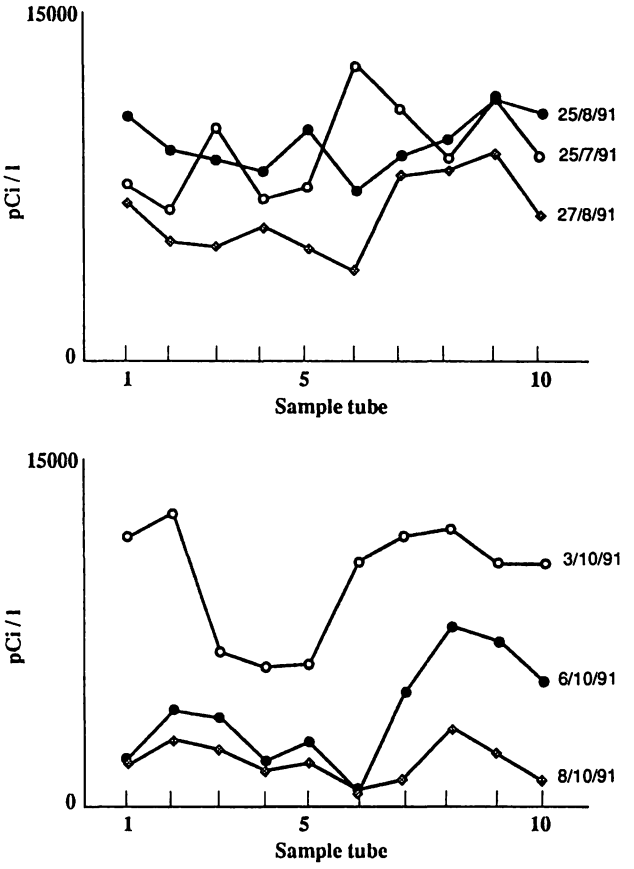

Fig. 7. Radon monitoring at site 217: Measurements of radon behavior at 10 sampling points at 3 + 3 different dates. The lines schematically connect all sampling tubes at a single date. Dates are given along graph.

The results are presented in Fig. 7. Each sampling set, i.e., the series of 10 sample tubes at a specific date of measurement, is denoted by a separate symbol. Six (3 + 3) time intervals are shown. Considerable differences are noted among the various sample points. However, with repeated sampling, it is found that the relative difference in radon concentration among the sampling points is retained. It is assumed that the variation between the points reflects the local geologic heterogeneity within the upper levels of the site. It can be expected that such heterogeneity has a considerable effect when such a high radon flux approaches the interface with the atmosphere, close to the surface. Therefore it may be that the maximum radon values represent the radon flow to the surface better than the average value.

The variability in average radon emanation (10 sampling points) over time is presented in Fig. 8. The sampling is, at this stage, unevenly spaced in time. Still, significant results are observed: Three or four peaks of the radon level of more than 9,000 pCi/l, 5 times higher than the local "background" level were observed. The last peak (at 20–24/10/91), which was traced throughout, spreads out over 10–14 days (base-level to base-level). An earlier peak value was just recorded some 20 days earlier.

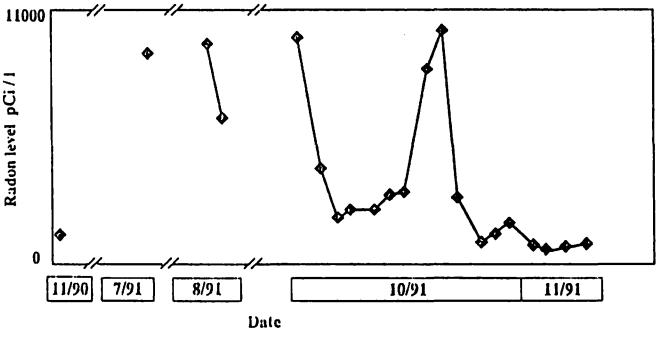

Fig. 8. Radon monitoring at site 217: Average radon level as a function of time (November 1990 to November 1991).

DISCUSSION AND CONCLUSIONS

Radon anomalies along the western shore of the Dead Sea, so far reported from geographically isolated springs in the area, are also traceable in the sediments and rock units. Some of these are in the vicinity of water sources, while others are removed from them. The anomalies are not supported by local uranium — i.e., in the rocks surrounding the sensors. Yet it is difficult to attribute them to local secondary radium concentrations. A "nonlocal" source must be called upon to explain the data.

The radon anomalies have been found at several areas along the western shore of the Dead Sea. The anomalies have a considerably greater spatial distribution than would have been suspected based upon the spring data. Thus it is also probable that they are abundant along this part of the Rift.

An individual radon anomaly can be traced over distances of up to 3 km along the strike (N–S) of the major structural elements and up to 1 km perpendicular to them (Fig. 9). In the anomaly the radon values reach up to 10 times the background values.

Superimposed upon these regional anomalies are intense local anomalies. Some of these are associated with "freshwater" springs flowing out from the young graben fill, not far from the Dead Sea shore. They are composed of a mixture of Dead Sea brine and freshwater. A second type of superimposed anomaly is related to the large N–S-trending faults. The latter are clearly defined major structural elements of the Rift. At these localities the radon anomaly itself is released in the Rift sediments adjoining the fault scarp.

Along the Dead Sea sector of the Rift, the radon anomalies are traced within the Rift proper. No radon anomalies occur over fault zones in the structural block immediately to the west of the main western fault of the Rift. This observation is supported by data obtained in a tunnel situated on the margin of the Rift at the southern part of the Dead Sea area (Fig. 1). The tunnel was excavated in the Judea Group carbonates, from the scarp of the main Rift fault, 600 m westward. The tunnel cuts subsidiary N–S faults of the Rift. Radon levels in the tunnel were measured at several localities, including positions on the faults. Only background radon values (Margaliot et al., 1991) were encountered. Systematic temporal fluctuations in the radon flux have been recorded at the very high radon anomaly at Enot Zuqim. The peak duration measured so far is on the order of 10 days. Such a variation precludes a near-surface secondary radium source for the radon. Similar temporal fluctuations in radon level also may have been detected at En Gedi Spa.

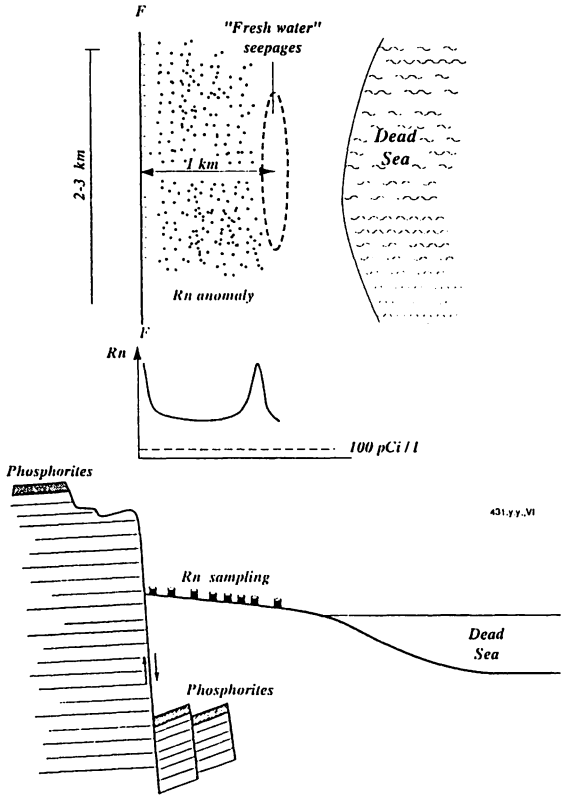

Fig. 9. Schematic representation (map and section) of a regional radon anomaly system.

The extent of the features observed suggests that in the investigated area a radon complex is developed governed by the interplay of three factors:

a. *A source rock emanating radon* at a very high level. The source is believed to extend over considerable stretches, at some as yet unknown depth. Judging by the size of the anomalies, and assuming a first-order relation of 1:1 between extension and depth to the source, the depth might be considerable. A likely source that could account for such release would be the Senonian phosphorite beds. Radon surveys indicate that high radon concentrations (up to 10,000 pCi/l) are released into the pore air of the phosphorite beds in the Negev (Shiloni et al., 1991). These beds, containing up to 100–120 ppm uranium, form a sequence, several tens of meters thick, developed in southern Israel and southern Jordan. There is no doubt that such strata are buried, due to down-

faulting, in the Dead Sea sector of the Rift. In the Judean Desert relics of the Senonian strata are observable close to the western scarp of the Dead Sea valley. This indicates that pre-Rift regional continental unconformities (Early–Middle Tertiary peneplains) did not erode them in this area. It is thus plausible that they are also existing on downfaulted blocks along the western boundary fault of the Dead Sea. The Late Senonian–Tertiary oil shale (stratigraphically slightly above the phosphate beds) outcrop in the downfaulted block at En Boqeq (Bentor and Vroman, 1960) serves as an example.

b. If a source can be assumed at depth, then a *transport mechanism* is needed to draw considerable amounts of radon rapidly upwards. Convective processes would be needed to account for the concentrations of radon encountered and the size of the anomalies as well as the indicated possible depth to the source. Such processes are also implied by the short (3.8 days) half-life involved.
c. A *conduit system* would be also needed to enable the transport of the radon from depth to the surface. Such a conduit system would be enhanced by the large border fault systems as well as by the active hydrologic systems existing along the Rift boundaries.

Summarizing, a formidable radon flux to the surface has been documented along major structural elements within a prominent tectonically active zone. To the best of our knowledge, such a combination has not been documented elsewhere.

Monitoring radon levels at selected sites has been suggested as one of the empirical approaches to earthquake prediction. This approach received attention since the observation of significant changes in episodic radon content in well-water prior to the Tashkent earthquake of 1966 (Ulomov and Mavashev, 1967). Since then, reports on anomalous changes in radon content in soils and groundwaters have been reported for several earthquakes from stations located at distances of tens and up to several hundred kilometers from the respective epicenters (cf. Ramola et al., 1989). The temporal behavior of radon anomalies and their usefulness in earthquake prediction has often been disputed. Wyss (1991) has recently stated that of all earthquake precursors so far suggested, success has only been demonstrated in some cases of radon monitoring. The results of this study suggest that the feasibility of radon monitoring as an earthquake precursor should be investigated in the Dead Sea area.

ACKNOWLEDGMENTS

This research was supported by the Earth Science Research Administration, Ministry of Energy and Infrastructure.

Y. Assael, Y. Yaffe, and O. Even are acknowledged for their contribution in all stages of the field work and analysis. Y. Yaffe assisted with the drafting.

This paper benefitted from constructive review comments, suggestions, and criticism by J. Kronfeld and E. Mazor.

REFERENCES

Agnon, A. 1983. The development of depositional basins and morphotectonics along the southern part of the western fault scarp of the Dead Sea. M. Sc. thesis, Hebrew Univ., Jerusalem, 61 p (in Hebrew).

Barretto, P.M.C. 1975. Radon-222 emanation characteristics of rocks and minerals. In: Radon in uranium mining, Panel proceedings, Washington D.C., IAEA STI/PUB/391, p 129–148.

Ben-Menachem, A. 1979. Earthquake catalog for the Middle East (92BC–1980AD). Boll. Geofis. Teor. Appl. 21: 245–313.

Bentor, Y.K., Vroman, A. 1960. The geological map of Israel 1:100,000, Sheet 16, Mount Sedom. 2nd edition. Geol. Surv. Isr. (with explanatory notes).

Durrance, E.M. 1986. Radioactivity in geology: principles and applications. (Ellis Horwood series in geology). New York: Wiley.

Fleischer, R.L., Price, P.B., Walker, R.M. 1975. Nuclear tracks in solids. University of California Press, Berkeley, California.

Fleischer, R.L., Hart, H.R., Mogro-Campero, A. 1980. Radon emanation over an ore body: search for long distance transport of radon. Nucl. Instrum. Methods 173: 169–181.

Gardosh, H. 1987. Stratigraphy and tectonic activity of the Late Quaternary in the Dead Sea basin.. M.Sc. thesis, Hebrew Univ., Jerusalem, 77 p (in Hebrew, English abstr.).

Garfunkel, Z., 1981. Internal structure of the Dead Sea leaky transform (rift) in relation to plate kinematics. Tectonophysics 80: 101–117.

Gingrich, J.E., Fisher J.C. 1976. Uranium exploration using the track etch methods. In: Exploration for uranium ore deposits (IAEA-SM-208/19). Vienna: International Atomic Energy Agency, p 213–228.

IRPG 1991. Earthquakes in and around Israel, 1990. Israel Institute Petroleum Research and Geophysics, Seismol. Bull. 9, 27 p.

Kristiansson, K., Malmqvist, L. 1982. Evidence for nondiffusive transport of Rn^{222} in the ground and a new physical model for the transport. Geophysics 47: 1441–1452.

Kristiansson, K., Malmqvist, L. 1984. The depth-dependence of the concentration of Rn^{222} in soil gas near the surface and its implication for exploration. Geoexploration 22: 17–41.

Kronfeld, J., Ilani S., Strull A. 1991. Radium precipitation and ^{238}U-series disequilibrium along the Dead Sea coast, Israel. Appl. Geochem. 6: 355–361.

Margaliot, M., Even, O., Schlesinger, T., Aharoni, A., Israeli, M. 1991. Radon concentrations in the tunnel of the Mediterranean–Dead Sea Project. Soreq Nuclear Research Center Rept. BK-5-1405, 14 p (in Hebrew).

Mazor, E. 1962. Radon and radium content of some Israeli water sources and a hypothesis on underground reservoirs of brines, oils and gases in the Rift Valley. Geochim. Cosmochim. Acta 26: 765–786.

Mogro-Campero, A., Fleischer R.L. 1980. Search for long–distance migration of subsurface radon. In: The natural environment. Rept. CONF-780422, U.S. Dept. of Energy, Washington, D.C., p 72–83.

Mor, U. 1987. The geology of the Judea Desert, Nahal Darga area. Geol. Surv. Isr. Rept. GSI/21/87, 112 p.

Pacer, J.C., Czarnecki R.F. 1982. Results of radon and helium surveys at three known uranium occurrences. In: Proc. Sympos. on Uranium Exploration Methods (Review of the NEA/IAEA R & D Programme), Paris, 1–4 June 1982. Paris: Nuclear Energy Agency, Organisation for Economic Co-operation and Development (OECD), p 517–528.

Papastefanou, C. Manolopoulou, M., Savvides, E., Charalambous, S. 1989. Radon monitoring at the Stivos Fault following the M_L = 6.5 earthquake which occurred at Thessaloniki, Greece on 20 June 1978. Nucl. Geophys. 3: 49–56.

Picard, L. 1943. Structure and evolution of Palestine (with comparative notes on neighbouring countries). Hebrew Univ., Jerusalem, Dept. Geol. Bull. 4(2–4), 187p.

Quennell, A.M. 1983. Evolution of the Dead Sea Rift — a review. In: Abed, A.M., Khalid, H., eds. Proc. First Jordan. Geol. Conf., Amman, Sept. 1982, p 69–483.

Ramola, R.C., Sandhu A. S., Singh M., Singh S., Virk H. S. 1989. Geochemical exploration of uranium using radon measurement techniques. Nucl. Geophys. 3(1): 57–70.

Rot, I. 1970. Geological map of Israel 1:50,000, Sheet Wadi El Qilt. Geol. Surv. Isr.

Shiloni, Y., Vulkan, U., Zafrir, H., Steinitz, G., Assael, Y., Yaffe, Y., Even, O. 1991. Radon in rock units in the northeastern Negev — activity for 1990/1991. Geol. Surv. Isr. Rept. TR-GSI/8/91 (in Hebrew).

Steinitz, G., Bartov, Y. 1991. The Miocene–Pleistocene history of the Dead Sea segment of the Rift in light of K-Ar ages of basalts. Isr. J. Earth Sci. 40: 199–208.

Steinitz, G., Vulkan, U., Lang, B., Gilat, A., Zafrir, H. 1992. Rn emanation along border faults of the Rift in the Dead Sea area — Progress report for 1991. Geol. Surv. Isr. Rept. GSI/35/91, 44 p.

Strull, A., Even, O., Assael, Y., Zafrir, H. 1986. New application of radon measurement by alpha-track technique over barren country rocks. Nuclear Soc. Isr. Annu. Mtg., 1986, p 134–138.

Tanner, A.B. 1964. Radon migration in the ground: A review. In: The natural radiation environment, Adams, J.A.S., Lowder, W.M., eds. Chicago: University of Chicago Press, p 161–190.

Tanner, A.B. 1980. Radon migration in the ground: A supplementary review. In: The natural radiation environment. Rept. CONF-780422, U.S. Dept. of Energy, Washington, D.C., p 5–56.

Turcotte, T., Arieh, E. 1986. Catalog of earthquakes in and around Israel. IRPG Rept. for the Israel Electric Corp. Ltd., 96 p.

Ulomov, V.I., Mavashev, B.Z. 1967. On fore-runners of strong earthquakes. Dokl. Akad. Nauk SSSR 176: 319 (in Russian).

Vulkan, U., Steinitz, G., Gilat, A., Lang, B., Yaffe, Y., Assael, Y., Even, O. 1991. Radon in rocks in the Dead Sea area — activity report for 1990–1991. Geol. Surv. Isr. Rept. TR-GSI/6/91, 12 p.

Wattananikorn, K., Asnachinda, P., Lamphunphong, S. 1990. Uranium exploration in the vicinity of abandoned fluorite mines, in northern Thailand, using cellulose nitrate films. Nucl. Geophys. 4(2): 253–258.

Wyss, M. 1991. Introduction. Tectonophysics 193: 253–254.